

PNC Enabled IIoT: A General Framework for Channel-Coded Asymmetric Physical-Layer Network Coding

Zhaorui Wang, Ling Liu, Shengli Zhang, Pengpeng Dong, Qing Yang, and Taotao
Wang

Abstract

This paper investigates the application of physical-layer network coding (PNC) to Industrial Internet of Things (IIoT) in which a controller and a robot are out of each other's transmission range, and they exchange messages with the assistance of a relay. We particularly focus on a scenario where the controller has more information to transmit, and the channel of the controller is stronger than that of the robot. To reduce the communication latency, we put forth an asymmetric PNC transmission scheme in which the controller and robot transmit different amount of information in the uplink of PNC simultaneously. The asymmetric transmission scheme is achieved through a way where the controller chooses a higher order modulation since the channel of the controller is stronger than that of the robot. To guarantee the transmission reliability, both users apply channel error correcting codes. A problem of the asymmetric transmission scheme is that a superimposed symbol at the relay contains different amount of source information from the controller and robot. It is thus hard for the relay to deduce meaningful network-coded messages by applying the current PNC decoding techniques which require the end users to transmit the same amount of information in the uplink of PNC. Currently, it still remains an open problem on the channel coding and modulation scheme design. To solve this problem, we propose a lattice based scheme in which the robot and controller encode and modulate their information in lattices with different lattice construction levels. Our design is versatile enough on that the controller and robot can freely choose their modulation orders based on their channel power, and the design is applicable for arbitrary channel error correcting codes, not just for one particular channel error correcting code. In addition, to make every dimension of the lattice power constrained, we apply hypercube power shaping. However, the hypercube power shaping causes decoding failures at the relay

Z. Wang is with the Department of Information Engineering, The Chinese University of Hong Kong, Hong Kong, China (e-mail: zrwang2009@gmail.com). L. Liu is with the College of Computer Science and Software Engineering, Shenzhen University, Shenzhen, China (e-mail: liulingcs@szu.edu.cn). S. Zhang, Q. Yang, and T. Wang are with the College of Electronics and Information Engineering, Shenzhen University, Shenzhen, China (e-mails: {zsl, yang.qing, ttwang}@szu.edu.cn). P. Dong is with Huawei Technologies Co., Ltd., Shanghai, China (e-mail: d47252@huawei.com). The corresponding author is S. Zhang.

since the hypercube power shaping is not a legal codeword to the channel error correcting codes in general. We solve this problem by asking the robot to transmit a correction signal beforehand such that the difference between the power shaping and the correction signal is a legal codeword. The simulation results demonstrate the effectiveness of the proposed asymmetric transmission scheme.

Index Terms

Physical layer network coding (PNC), industrial internet of things (IIoT), lattice, polar codes.

I. INTRODUCTION

In this paper, we focus on a scenario in Industrial Internet of Things (IIoT) where a controller and a robot are out of each other's transmission range, and they exchange messages with the assistance of a relay [1]–[4]. To achieve the stringent requirement on the communication latency between the robot and controller in IIoT, we apply physical layer network coding (PNC) [5], [6], as shown in Fig. 1. Specifically, at time slot 1, the controller and robot transmit their messages simultaneously to the relay. From the overlapped signals, the relay deduces a network-coded message. At time slot 2, the relay broadcasts the network-coded message to the controller and robot. The robot then uses the network-coded message and its own message to deduce the message from the controller. Likewise for the controller. Compared with the traditional scheme which requires four times slots for the communications between the robot and controller, PNC can reduce the communication latency from four time slots to two time slots [5]–[7].

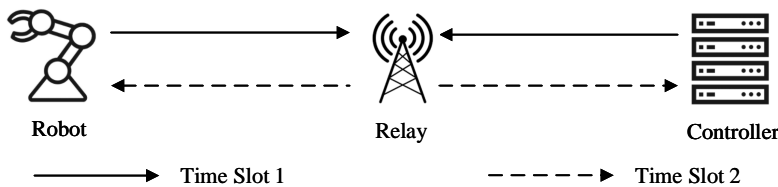


Fig. 1. A controller and a robot are out of each other's transmission range, and they exchange messages with the assistance of a relay. The PNC technique is applied to reduce the communication latency.

Within the robot and controller communication scenario, we are particularly interested in the case where 1) the message length from the controller is larger than that from the robot. For example, the controller controls motion of the robot through a series of instructions, and the robot only needs to feed back a one-bit acknowledgment to indicate if the robot executes the motion accordingly to the controller; 2) the channel power between the controller and relay, is stronger than that between the robot and relay. For example, the channel between the controller and relay is a line-of-sight channel, while the channel between the robot and relay is a non-line-of-sight channel due to the equipment

around the robot. In the most of current PNC studies, the uplink of PNC requires that the robot and controller transmit the same length of information even in the case where the channel power between the controller and relay is stronger than that between the robot and relay [8]–[10]. In this case, the controller should find another time slot to transmit the rest of information separately. Specifically, let K_R denote the information length of the robot, and $K_C > K_R$ denote the information length of the controller. In the uplink of PNC stage, the robot and controller both transmit K_R -length information to the relay. Then, the controller transmits the rest of $(K_C - K_R)$ -length information to the relay separately. We name this transmission strategy as “symmetric transmission scheme”.

In this paper, by exploiting the large channel power at the controller, we put forth an “asymmetric transmission scheme” where the controller transmits K_C -length information and the robot transmits K_R -length information to the relay simultaneously in the uplink of PNC. Since the controller exploits the channel power to transmit much more information in the uplink of PNC, the time for the transmission of $(K_C - K_R)$ -length information in the symmetric transmission scheme is reduced. To guarantee the transmission reliability in the asymmetric transmission scheme, channel error correcting codes are necessary. A key challenge is how to do channel coding and modulation in asymmetric PNC transmission. For example, the robot transmits a QPSK modulated packet. Since the channel between the controller and relay is stronger, we assume that the controller transmits a 8-QAM modulated packet. In addition, the robot and controller apply a same channel error correcting code. Since each QPSK symbol contains 2 encoded bits of the codeword from the robot, while each 8-QAM symbol contains 3 encoded bits of the codeword from the controller, it is hard for the relay to find a channel decoder to deduce meaningful network-coded messages from the superimposed packet from the controller and robot.

A. Related Work

Prior to this work, [11], [12] put forth novel channel coding and modulation schemes to solve the problem partially in asymmetric PNC transmission. First, the channel coding and modulation scheme in [11] is applied to the case where the robot applies BPSK modulation, and the controller applies QPSK modulation. The channel coding and modulation scheme in [12] can be applied to the case where the robot applies 2^m -QAM modulation, and the controller applies 2^{2m} -QAM modulation, $m \geq 1$. Second, the channel coding and modulation scheme in [11] is designed particularly for repeat-accumulate (RA) codes, and channel coding and modulation scheme in [12] is designed particularly for convolutional codes. It still remains an open problem on the channel coding and modulation scheme in which the robot and controller can freely choose their modulation schemes and channel

error correcting codes, e.g., the robot applies QPSK modulation, and the controller applies 8-QAM modulation according to their corresponding channel power, and they both apply polar codes. In this paper, we put forth a general framework to solve the above problem comprehensively. The detailed description of the encoding and modulation schemes in [11], [12] is shown in Section II-D.

B. Contributions

First, we put forth an asymmetric transmission scheme to reduce the communication latency between the controller and the robot. As we show above, compared with the symmetric transmission scheme, the proposed asymmetric transmission scheme can potentially save the time for the transmission of $(K_C - K_R)$ -length information.

Second, we put forth a lattice based channel encoding and modulation framework to solve the problem arising from the controller and robot transmitting different amount of information in the uplink of PNC transmission. Specifically, a lattice is a discrete set of points in a complex Euclidean space that forms a group under ordinary vector addition [13]. The lattice can be constructed through a set of nested linear binary channel codes $\mathcal{C}_1 \subseteq \mathcal{C}_2 \subseteq \dots \subseteq \mathcal{C}_{L-1}$, and a power shaping at the lattice level L , where \mathcal{C}_l lies in the l -th level of the lattice, $l = 1, \dots, L - 1$, and L is the number of lattice construction level. The power shaping constrains the power of the lattice, and the lattice with different L has different power. In this case, the lattice level L corresponds to the modulation order. In short, the lattice encoding combines the channel encoding and modulation to a joint process. In addition, we can extract the binary channel codes \mathcal{C}_l separately from the lattice, $l = 1, \dots, L - 1$.

In the uplink of PNC transmission, we propose to ask controller and robot to encode and modulate their information through lattices. The number of lattice level depends on their channel power. Denote the number of lattice level at the robot and controller by L_R and L_C , respectively. Since the channel at the controller is stronger, we have $L_C > L_R$. In addition, the lattices from the controller and robot should be constructed through a same set of nested binary channel codes $\mathcal{C}_1 \subseteq \mathcal{C}_2 \subseteq \dots \subseteq \mathcal{C}_{L_C-1}$. The relay receives a superimposed lattice from the two users with different modulation orders, i.e., number of lattice levels. Since the relay can extract the binary codes at each level of the received lattice, and the codes at the each level of the lattice from the controller and robot are the same, the relay can estimate the network-coded message at the each level of the received lattice. In this case, although the controller and robot have different amount of information, they encode their information through lattices with different construction levels. The relay can thus successfully estimate the network-coded messages from the received lattice level-by-level. Our design is versatile enough on that the controller and robot can freely choose their modulation orders based on their channel power, and the design

is applicable for arbitrary channel error correcting codes, not just for one particular channel error correcting code.

Third, to make the every dimension of transmitted lattice power constrained, we apply hypercube power shaping [14]. However, since the hypercube power shaping is not a legal codeword to the codes \mathcal{C}_{L_R} in general, the channel decoder at the lattice level L_R can not decode network-coded information successfully, which then causes decoding error propagation at the lattice levels $l > L_R$. To solve this problem, we ask the robot to transmit a correction signal beforehand, such that the difference between the power shaping and the correction signal is a legal codeword to the codes \mathcal{C}_{L_R} . Upon receiving the superimposed signal, the correction signal is subtracted from the received signal. In this case, the decoder at the relay can estimate the network-coded messages successfully.

Last, to reduce the correction signal transmission time, we apply the polar source coding [15], [16] technique to compress the correction signal and we transmit the compressed correction signal instead. We find that the polar source coding technique can efficiently reduce the correction signal transmission time when the channel coding rate at lattice level L_R is close to 1. We emphasize that this can be achieved when the lattice construction level is large. In the numerical section, we show this through an example when $L_C = 5$, i.e., the modulation order is 4. To make the study of the asymmetric transmission comprehensive, we also consider the case where channel coding rate at lattice level L_R is not close to 1. In this case, the length of the compressed correction signal may be large, and the asymmetric transmission scheme may spend much time on the correction signal transmission in addition to the PNC transmission. Thus, the overall asymmetric transmission time may be larger than the symmetric transmission time. To solve this problem, we put forth a dynamic transmission scheme in which the relay dynamically selects one of the transmission schemes which has smaller transmission time.

C. Organization

The rest of this paper is organized as follows. Section II describes the system model for the symmetric transmission scheme and asymmetric transmission scheme. In addition, we detail the related work on the channel encoder and modulator in asymmetric transmission scheme in Section II-D. Section III introduces the proposed lattice-based channel encoder and modulator in asymmetric transmission, and the power shaping design. Section IV presents the numerical results to validate the effectiveness of the proposed asymmetric transmission scheme. Section V proposes a dynamic transmission scheme to solve the problem on which the symmetric transmission time may be smaller than that of the asymmetric transmission. Finally, Section VI concludes this paper.

II. SYSTEM MODEL

In this paper, we study the communications between a controller and a robot in a two way relay channel (TWRC), as shown in Fig. 1. The controller and robot are out of each other's transmission range, and they exchange messages with the assistance of a relay. In particular, we focus on a scenario in which the channel between the controller and relay is stronger than that of the robot, and the controller has much information to transmit than the robot. Specifically, we denote the robot by A , the controller by B , and the relay by R to simplify the exposition. In addition, let h_u be the channel between user u and relay R , $u \in \{A, B\}$. From the assumption above, we have $|h_B| > |h_A|$. We assume that the coherence time is larger than a packet duration, and thus h_u keeps constant within a packet duration, $u \in \{A, B\}$. In addition, given the same transmit power and channel coding rate, for a target frame error rate (FER), a channel with stronger power can support a higher modulation order [17]. Suppose the signal modulation order that can be supported by the channel h_u is M_u , $u \in \{A, B\}$. In this case, we have $M_B > M_A$. Let $s_u \in \{0, 1\}^{K_u}$ denote the source information of user u , where K_u is the length of the source information, $u \in \{A, B\}$. Under the considered setup, we have $K_B > K_A$. Note that, most of the current PNC studies require that the users A and B apply the same coding rate and modulation order [10], [18]–[22]. To achieve this, [10], [18]–[22] require the source information length at both users should be equal to each other, i.e., $K_A = K_B$. To reduce the transmission duration, in this paper, we put forth an asymmetric transmission scheme in which the both users can transmit different amount of source information, i.e., $K_B \neq K_A$. We use the case $K_B > K_A$ to show our design in the rest of this paper.

A. Symmetric Transmission Scheme

We first consider the symmetric transmission scheme, in which the both users A and B transmit source information with the same length during the PNC phase, and user B transmits the rest of information separately in the point-to-point (P2P) phase. The signal transmission process is detailed as follows.

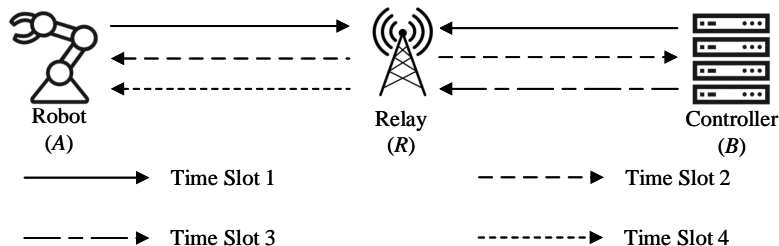


Fig. 2. Symmetric transmission scheme where the whole transmission takes four time slots.

Time slot 1: Uplink PNC transmission. The source information \mathbf{s}_B from user B is divided into the two parts: $\mathbf{s}_{B,PNC}$ and $\mathbf{s}_{B,P2P}$, where $\mathbf{s}_{B,PNC} \in \{0, 1\}^{K_A}$, and $\mathbf{s}_{B,P2P} \in \{0, 1\}^{(K_B - K_A)}$. The information $\mathbf{s}_{B,PNC}$ is transmitted during the PNC phase, and the information $\mathbf{s}_{B,P2P}$ is transmitted by user B separately during the P2P phase. In the PNC phase, the source information \mathbf{s}_A and $\mathbf{s}_{B,PNC}$ with the same length go through a same channel-encoder-and-modulator, with coding rate $R_{A,PNC} = R_{B,PNC}$, and modulation order M_A . Note that the modulation order now is restricted by the weaker channel h_A . The transmitted packets are $\mathbf{x}_{A,PNC}$ and $\mathbf{x}_{B,PNC}$, respectively. We assume that the bandwidth in the uplink and downlink channel is W symbols per second, i.e., the transmitter transmits W modulated symbols to the receiver per second. The time slot 1 duration is

$$T_1^{(Sym)} = \frac{K_A}{R_{A,PNC} M_A W}. \quad (1)$$

We assume that the signals from users A and B arrive at relay R simultaneously, the received signal is expressed as:

$$\mathbf{y}_{R,PNC} = h_A \frac{1}{\sqrt{p_A}} \beta_A \mathbf{x}_{A,PNC} + h_B \frac{1}{\sqrt{p_B}} \beta_B \mathbf{x}_{B,PNC} + \mathbf{n}_{R,PNC}, \quad (2)$$

where $\frac{1}{\sqrt{p_u}}$ is the symbol power normalization factor at user u , β_u is the channel precoder to compensate the channel at user u , $u \in \{A, B\}$, and $\mathbf{n}_{R,PNC} \sim \mathcal{CN}(\mathbf{0}, \sigma_{R,PNC}^2 \mathbf{I})$ denotes the additive white Gaussian noise (AWGN) at the relay. In addition, we assume perfect channel precoding at the users, i.e.,

$$h_u \frac{1}{\sqrt{p_u}} \beta_u = 1, \quad u \in \{A, B\}. \quad (3)$$

The channel precoding technique has been studied and implemented in [14]. In this case, (2) becomes

$$\mathbf{y}_{R,PNC} = \mathbf{x}_{A,PNC} + \mathbf{x}_{B,PNC} + \mathbf{n}_{R,PNC}. \quad (4)$$

Based on the received signals \mathbf{y}_R , the relay R deduces network-coded messages from users A and B . Note that, since users A and B applies a same channel-encoder-and-modulator, the current PNC decoder-and-demodulator [20]–[22] can be applied directly. The estimated network-coded information is denoted by $\mathbf{s}_{R,PNC} \in \{0, 1\}^{K_A}$.

Time slot 2: Downlink PNC transmission. The relay then broadcasts the estimated network-coded information to both end users. The relay applies a channel-encoder-and-modulator, with coding rate $R_{R,PNC}$ and modulation order M_A . The modulation order is restricted by the weaker channel h_A to achieve a target FER for the two users. In addition, for exposition simplicity, we assume that the modulation order in time slot 2 is the same as that in time slot 1, and the downlink PNC can

achieve different FERs by adjusting the coding rate $R_{R,PNC}$. The broadcast packet is $\mathbf{x}_{R,PNC}$, and the duration of the time slot 2 is

$$T_2^{(Sym)} = \frac{K_A}{R_{R,PNC}M_AW}. \quad (5)$$

At the user u , the received signal from the relay is

$$\mathbf{y}_{u,PNC} = \mathbf{x}_{R,PNC} + \mathbf{n}_{u,PNC}, u \in \{A, B\}, \quad (6)$$

where $\mathbf{n}_{u,PNC} \sim \mathcal{CN}(\mathbf{0}, \sigma_{u,PNC}^2 \mathbf{I})$ denotes the additive white Gaussian noise (AWGN) at the user u in the PNC phase. Note that, the channel h_u has been compensated at user u . The decoder at user u decodes the messages from the other user based on the received signal $\mathbf{y}_{u,PNC}$ and its own message \mathbf{x}_u .

Time slot 3: User B uplink P2P transmission. User B transmits its remaining information $\mathbf{s}_{B,P2P}$ with length $(K_B - K_A)$. The user B applies a channel-encoder-and-modulator with coding rate $R_{B,P2P}$. In addition, since the channel between user B and the relay is stronger than that between user A and the relay, the modulation order now is assumed to be M_B . The transmitted packet is $\mathbf{x}_{B,P2P}$, and the duration of the time slot 3 is

$$T_3^{(Sym)} = \frac{K_B - K_A}{R_{B,P2P}M_BW}. \quad (7)$$

At the relay R , the received signal is

$$\mathbf{y}_{R,P2P} = \mathbf{x}_{B,P2P} + \mathbf{n}_{R,P2P}, \quad (8)$$

where $\mathbf{n}_{R,P2P} \sim \mathcal{CN}(\mathbf{0}, \sigma_{R,P2P}^2 \mathbf{I})$ denotes the additive white Gaussian noise (AWGN) at the relay in the P2P phase. Note that, the channel h_B has been compensated at the relay. The decoder at the relay R decodes the messages from user B based on the received signal $\mathbf{y}_{R,P2P}$. The estimated information is denoted by $\mathbf{s}_{R,P2P} \in \{0, 1\}^{(K_B - K_A)}$.

Time slot 4: Relay R downlink P2P transmission. The relay then transmits the information $\mathbf{s}_{R,P2P}$ to user A . The relay R applies a channel-encoder-and-modulator with coding rate $R_{R,P2P}$, and the modulation order M_A . The modulation order is restricted by the channel h_A . In addition, for exposition simplicity, we assume that the modulation order in time slot 4 is the same as that in time slots 1 and 2, and the downlink P2P can achieve different FERs by adjusting the coding rate $R_{R,P2P}$. The duration of time slot 4 is

$$T_4^{(Sym)} = \frac{K_B - K_A}{R_{R,P2P}M_AW}. \quad (9)$$

At the user A , the received signal is

$$\mathbf{y}_{A,P2P} = \mathbf{x}_{R,P2P} + \mathbf{n}_{A,P2P}, \quad (10)$$

where $\mathbf{n}_{A,P2P} \sim \mathcal{CN}(\mathbf{0}, \sigma_{A,P2P}^2 \mathbf{I})$ denotes the additive white Gaussian noise (AWGN) at user A in the P2P phase. Note that, the channel h_A has been compensated at user A . The decoder at the user A decodes the messages from user B based on the received signal $\mathbf{y}_{A,P2P}$.

Overall, the transmission time in the symmetric transmission scheme is

$$\begin{aligned} T^{(Sym)} &= T_1^{(Sym)} + T_2^{(Sym)} + T_3^{(Sym)} + T_4^{(Sym)} \\ &= \frac{K_A}{R_{A,PNC}M_AW} + \frac{K_A}{R_{R,PNC}M_AW} + \frac{K_B - K_A}{R_{B,P2P}M_BW} + \frac{K_B - K_A}{R_{R,P2P}M_AW}. \end{aligned} \quad (11)$$

B. Asymmetric Transmission Scheme

A problem in the symmetric transmission scheme is that, in the uplink PNC phase (i.e., time slot 1 in the symmetric transmission), user B transmits signals with a lower modulation order M_A , although the channel power between user B and the relay can support user B to transmits signals with a higher modulation order $M_B > M_A$. This takes user B additional time for signal transmission. In this paper, by exploiting the stronger channel at user B , we put forth an asymmetric transmission scheme, in which user A transmits its K_A -length source information, and user B transmits its K_B -length source information simultaneously during the uplink of PNC phase. The signal transmission processes are detailed as follows.

Time slot 1: Uplink PNC transmission. User A transmits its source information \mathbf{s}_A , and user B transmits its source information \mathbf{s}_B to the relay at the same time. The source information \mathbf{s}_A goes through a channel-encoder-and-modulator with coding rate $R_{A,PNC}$ and modulation order M_A , and the transmitted packet is $\mathbf{x}_{A,PNC}$; the source information \mathbf{s}_B goes through a channel-encoder-and-modulator with coding rate $R_{B,PNC}$. The coding rate $R_{B,PNC}$ should be chosen roughly the same as the rate $R_{A,PNC}$. In this case, since the channel from user B is stronger than that of user A , the modulation order at user B now is $M_B > M_A$. Note that, both users should apply a same type of channel error correcting code, such as polar codes, convolutional codes, or LDPC codes. The transmitted packet is $\mathbf{x}_{B,PNC}$. We assume that the lengths of source information from the two users are chosen such that the lengths of the transmitted packets from the two users are the same. The time slot 1 duration is

$$T_1^{(Asy)} = \frac{K_A}{R_{A,PNC}M_AW} = \frac{K_B}{R_{B,PNC}M_BW}. \quad (12)$$

The received signal at the relay is the same as that shown in (4). A key challenge is how to design a channel-encoder-and-modulator at the two users such that the relay can decode the network-coded messages from the two end users. We will show our design on the encoder and decoder in Section III. The estimated network-coded information is denoted by $\mathbf{s}_{R,PNC} \in \{0, 1\}^{K_B}$.

Time slot 2: Downlink PNC transmission. The relay then broadcasts the estimated network-coded information to the two end users. The relay applies a channel-encoder-and-modulator, with coding rate $R_{R,PNC}$ and modulator order M_A . The modulator order is restricted by the weaker channel h_A to achieve a targeted FER. In addition, the modulation order is the same as that in time slots 2 and 4 in the symmetric transmission scheme in order to have a fair transmission time comparison later. The broadcast packet is $\mathbf{x}_{R,PNC}$, and the duration of the time slot 2 is

$$T_2^{(Asy)} = \frac{K_B}{R_{R,PNC}M_AW}. \quad (13)$$

The received signal at the relay is the same as that shown in (6). The decoder at user u decodes the messages from the other user based on the received signal $\mathbf{y}_{u,PNC}$ and its own message \mathbf{x}_u , $u \in \{A, B\}$.

Overall, the transmission time in the asymmetric transmission scheme is

$$T^{(Asy)} = T_1^{(Asy)} + T_2^{(Asy)} = \frac{K_A}{R_{A,PNC}M_AW} + \frac{K_B}{R_{R,PNC}M_AW}. \quad (14)$$

If we set $R_{R,PNC} = R_{R,P2P}$, from (11) and (14), we have

$$T^{(Sym)} - T^{(Asy)} = T_3^{(Sym)} = \frac{K_B - K_A}{R_{B,P2P}M_BW}. \quad (15)$$

Equ. (15) shows that the time slot 3 in symmetric transmission scheme is saved by the asymmetric transmission scheme.

C. Challenge in Traditional Channel-Encoder-and-Modulator in Asymmetric Transmission

We first show the traditional channel-encoder-and-modulator, i.e., the channel-encoder-and-modulator applied in the current PNC systems, and its problems when applied to asymmetric transmission scheme through a concrete example. In time slot 1 of the asymmetric transmission scheme shown in Section II-B, the source information \mathbf{s}_u first goes through a channel encoder, the output codeword is \mathbf{c}_u with codeword length D_u , $u \in \{A, B\}$. Suppose that the codeword length $D_B = 2D_A$. Then, the codeword \mathbf{c}_A goes through a BPSK modulator, and \mathbf{c}_B goes through a QPSK modulator. As a result, the modulated packets $\mathbf{x}_{A,PNC}$ and $\mathbf{x}_{B,PNC}$ have the same length. The problem is, since each BPSK symbol within $\mathbf{x}_{A,PNC}$ contains 1 encoded bit of the codeword \mathbf{c}_A , while each QPSK symbol within $\mathbf{x}_{B,PNC}$ contains 2 encoded bits of the codeword \mathbf{c}_B , it is hard for the relay R to

find a channel decoder to deduce meaningful network-coded messages from the superimposed packet between $\mathbf{x}_{A,PNC}$ and $\mathbf{x}_{B,PNC}$. In this case, the above traditional channel-encoder-and-modulator is not applicable to the asymmetric transmission in PNC.

D. Related Work on Channel-Encoder-and-Modulator in Asymmetric Transmission

Prior to this work, [11], [12] put forth novel schemes to solve the above problem. Specifically, in [11], user A follows the traditional channel-encoder-and-modulator shown in Section II-C, and the modulated packet is $\mathbf{x}_{A,PNC} \in \{-1, 1\}^N$, where N is the packet length. To solve the problem detailed in Section II-C, user B divides the source information \mathbf{s}_B into the following two parts: $\mathbf{s}_{B,1}$ and $\mathbf{s}_{B,2}$, where $\mathbf{s}_{B,i} \in \{0, 1\}^{K_{B,i}}$, $i = 1, 2$. In [11], $K_{B,1} = K_{B,2} = K_A$. The source information $\mathbf{s}_{B,1}$ and $\mathbf{s}_{B,2}$ first go through a same RA channel encoder, and the output codewords are $\mathbf{c}_{B,1}$ and $\mathbf{c}_{B,2}$, respectively. Then, the codewords $\mathbf{c}_{B,1}$ and $\mathbf{c}_{B,2}$ go through a BPSK modulator separately, and the output BPSK packets are $\mathbf{x}_{B,PNC}^I \in \{-1, 1\}^N$ and $\mathbf{x}_{B,PNC}^Q \in \{-1, 1\}^N$, respectively. Finally, the QPSK modulated packet of user B is:

$$\mathbf{x}_{B,PNC} = \mathbf{x}_{B,PNC}^I + j\mathbf{x}_{B,PNC}^Q, \quad (16)$$

where $j^2 = -1$. In this case, the scheme makes two BPSK modulated packets $\mathbf{x}_{B,PNC}^I$ and $\mathbf{x}_{B,PNC}^Q$ embedded in the in-phase and quadrature parts of one QPSK modulated packet $\mathbf{x}_{B,PNC}$, respectively. Since each BPSK symbol within $\mathbf{x}_{A,PNC}$, $\mathbf{x}_{B,PNC}^I$, and $\mathbf{x}_{B,PNC}^Q$ all contains 1 encoded bit information of their corresponding codewords, the traditional channel decoder can be applied to deduce the network-coded messages at the relay. The relay in [11] applies a PNC joint channel decoder. Specifically, [11] first jointly decodes \mathbf{s}_A , $\mathbf{s}_{B,1}$, and $\mathbf{s}_{B,2}$ based on the received signal $\mathbf{y}_{R,PNC}$ in (4). Then, the network-coded message $\mathbf{s}_{R,PNC}$ is as follows:

$$\mathbf{s}_{R,PNC} = [\mathbf{s}_A \oplus \mathbf{s}_{B,1}, \mathbf{s}_A \oplus \mathbf{s}_{B,2}], \quad (17)$$

where \oplus denotes the XOR operation. Ref. [11] shows the scheme where user A applies BPSK modulation, and user B applies QPSK modulation. It is not clear whether the channel encoding and modulation scheme in [11] can be extended to the cases beyond BPSK-QPSK combination. The following three factors make the extension difficult:

- *Channel decoder design issue*: The channel decoder at the relay is particularly designed for RA codes. We should re-design the channel decoder if another channel code is applied. In addition, the PNC joint channel decoder applied in [11] is not widely used due to the decoding complexity issue. Specifically, the decoding complexity increases as the number of input states to the channel

decoder. In the above example, the input states is $2^{(1+2)} = 8$. The number of input states of the scheme exponentially increase with the sum of the modulation orders from the two users, making the joint channel decoder infeasible to high order modulations.

- *PNC XOR mapping issue*: It is not clear how to do PNC XOR mapping beyond the BPSK-QPSK combination.

We next introduce the channel-encoder-and-modulator in [12]. Specifically, the channel-encoder-and-modulator in [12] is the same as that in [11] introduced above except that the convolutional code is applied in [12]. In addition, [12] applies a PNC XOR channel decoder. Specifically, [12] first applies the PNC XOR mapping between codewords as follows:

$$\mathbf{c}_{R,PNC} = [\mathbf{c}_A \oplus \mathbf{c}_{B,1}, \mathbf{c}_A \oplus \mathbf{c}_{B,2}]. \quad (18)$$

Then, the soft information of $\mathbf{c}_{R,PNC}$ in (18) is fed to the channel decoder to get the network-coded message in (17). Ref. [12] use the same way to deal with the other cases beyond BPSK-QPSK combination. The problems are 1) according to the PNC mapping in (18), the codeword length of user B should always be two times as much as that of user A . Thus, the scheme from [12] can only be applied to the case where user A applies 2^m -QAM modulation, and user B applies 2^{2m} -QAM modulation, $m \geq 1$; 2) The channel decoder at the relay is particularly designed for convolutional codes. We should re-design the channel decoder if another channel code is applied.

In general, the channel-encoder-and-modulator in [11], [12] cannot be generally applied to the cases in which users A and B can freely choose their channel codes, and modulation schemes according to their channel power, e.g., user A applies QPSK modulation, and user B applies 8-QAM modulation with low decoding complexity. In the following, we put forth a lattice-based channel-encoder-and-modulator to solve the above problem comprehensively.

III. LATTICE-BASED CHANNEL-ENCODER-AND-MODULATOR IN UPLINK OF ASYMMETRIC PNC

In Section II-B, we propose an asymmetric transmission scheme to improve the throughput of the PNC systems. To achieve this, users A and B should apply different coding and modulation strategies such that they can transmit different amount of information in the uplink of PNC. A key challenge is how to design the channel-encoder-and-modulator at the two users such that the relay can decode the network-coded messages from the two users. In this section, we propose a lattice-based channel-encoder-and-modulator to solve the above problem.

A. Preliminaries for Lattice

A complex lattice Λ_1 is a discrete set of points in a complex Euclidean n -dimensional space \mathbb{C}^n that forms a group under ordinary complex vector addition, $n \geq 1$ [13]. A sublattice Λ_2 ($\Lambda_2 \subseteq \Lambda_1$) induces a partition of Λ_1 into equivalence groups modulo Λ_2 . We denote this partition by Λ_1/Λ_2 . When the number of cosets of Λ_2 in Λ_1 is two, the lattice partition is the binary lattice partition. Let $\Lambda_1/\Lambda_2/\dots/\Lambda_{L-1}/\Lambda_L$ denote an n -dimensional lattice partition chain for $L \geq 2$. For each partition Λ_l/Λ_{l+1} , a code \mathcal{C}_l over Λ_l/Λ_{l+1} selects a sequence of coset representatives $a_l \in A_l$, where A_l is a set that contains all the coset representatives of Λ_{l+1} in the partition Λ_l/Λ_{l+1} , $1 \leq l \leq L-1$. The construction of the binary lattice requires a set of nested linear binary codes \mathcal{C}_l with codeword length D and source information length k_l , $l = 1, \dots, L-1$, and $\mathcal{C}_1 \subseteq \mathcal{C}_2 \subseteq \dots \subseteq \mathcal{C}_{L-1}$. Let π be the natural embedding of \mathbb{F}_2^D into \mathbb{Z}^D , where \mathbb{F}_2^D is the binary field. In addition, let $\mathbf{e}_1, \mathbf{e}_2, \dots, \mathbf{e}_{k_l}$ be a basis of \mathbb{F}_2^D that spans the code \mathcal{C}_l . When $n = 2$, a vector \mathbf{x} in the binary lattice is expressed as

$$\mathbf{x} = \sum_{l=1}^{L-1} \phi^{l-1} \sum_{j=1}^{k_l} \alpha_j^{(l)} \pi(\mathbf{e}_j) + \phi^{L-1} \mathbf{b}, \quad (19)$$

where $\phi = 1 + j$, $\alpha_j^{(l)} \in \{0, 1\}$, and $\mathbf{b} \in \mathbf{G}^D$ with \mathbf{G} being a set of Gaussian integers. Moreover, the length of \mathbf{x} now is $N = D$. Furthermore, if \mathbf{x} is a baseband transmitted signal, the above lattice construction system combines the channel coding and modulation as a joint process, which is quite different from the traditional channel-encoder-and-modulator with separated channel coding and modulation processes. In addition, the power shaping \mathbf{b} should be carefully chosen such that the transmitted baseband signal \mathbf{x} is power constrained. We will detail this in Section III-C.

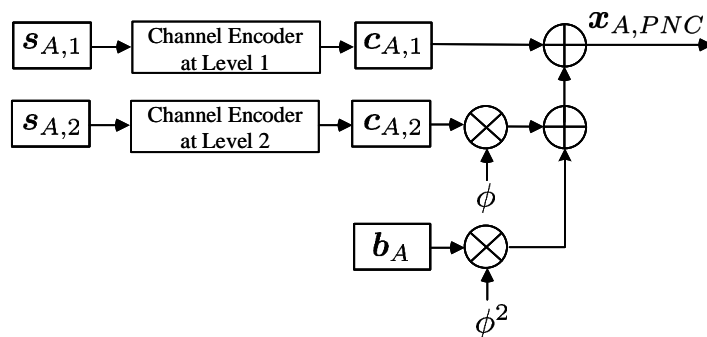


Fig. 3. A lattice-based channel-encoder-and-modulator at user A when $L_A = 3$.

B. Lattice-based Encoder and Decoder

Now, we show the lattice constructions at users A and B in the uplink of PNC. The lattice construction at both users strictly follows the description in Section III-A. Specifically, according to the channel power, user u applies L_u levels lattice construction, $u \in \{A, B\}$. Then, user u first

divides the source information \mathbf{s}_u as $\mathbf{s}_u = [\mathbf{s}_{u,1}, \dots, \mathbf{s}_{u,L_u-1}]$, where $\mathbf{s}_{u,l}$ with length $K_{u,l}$ is the source information at level l in the lattice, $l = 1, \dots, L_u - 1$, and $u \in \{A, B\}$. Next, at level l , we apply a channel encoder with coding rate $R_{u,l}$ to encode the source information $\mathbf{s}_{u,l}$, and the output codeword is $\mathbf{c}_{u,l} \in \mathbb{Z}^{D_u}$, where D_u is the codeword length, $R_{u,1} \leq R_{u,2} \leq \dots \leq R_{u,L_u-1}$, $u \in \{A, B\}$, and $l = 1, \dots, L_u - 1$. Note that, both users should apply a same type of channel error correcting code, e.g., polar codes, LDPC codes, or convolutional codes, during the lattice construction. In addition, the source information length and coding rate at each level of lattice should be the same for the two users, i.e., $K_{A,l} = K_{B,l}$, and $R_{A,l} = R_{B,l} = R_l, \forall l$. As a result, we have $D_A = D_B$. Finally, the transmitted packet $\mathbf{x}_{u,PNC}$, $u \in \{A, B\}$, is expressed as:

$$\mathbf{x}_{u,PNC} = \mathbf{c}_{u,1} + \phi \mathbf{c}_{u,2} + \dots + \phi^{L_u-2} \mathbf{c}_{u,L_u-1} + \phi^{L_u-1} \mathbf{b}_u. \quad (20)$$

The length of the transmitted packet $\mathbf{x}_{u,PNC}$ is $N = D_A = D_B$. We will show how to design the power shaping \mathbf{b}_u later in Section III-C. In addition, in Fig. 3, we show a illustrative example of the lattice-based channel-encoder-and-modulator at user A when $L_A = 3$.

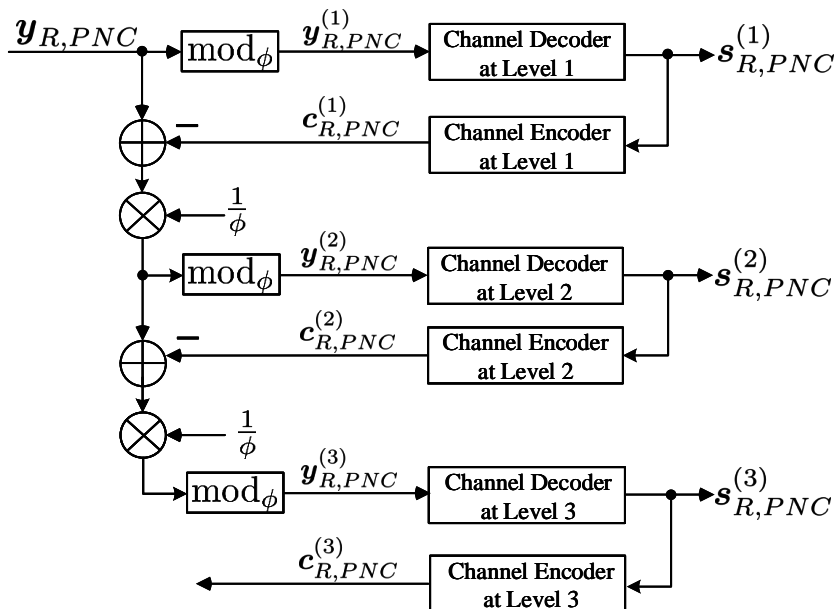


Fig. 4. A decoder at relay R when $L_A = 3$ and $L_B = 4$.

Next, we introduce the decoder at relay R . According to (4), the received signal at the relay is

$$\begin{aligned} \mathbf{y}_{R,PNC} &= \mathbf{x}_{A,PNC} + \mathbf{x}_{B,PNC} + \mathbf{n}_{R,PNC} \\ &= (\mathbf{c}_{A,1} + \mathbf{c}_{B,1}) + \dots + \phi^{L_A-2} (\mathbf{c}_{A,L_A-1} + \mathbf{c}_{B,L_B-1}) \\ &\quad + \phi^{L_A-1} (\mathbf{b}_A + \mathbf{c}_{B,L_A}) + \dots + \phi^{L_B-1} \mathbf{b}_B + \mathbf{n}_{R,PNC}. \end{aligned} \quad (21)$$

From (21), the effective signals $\mathbf{x}_{A,PNC} + \mathbf{x}_{B,PNC}$ forms a L_B levels lattice at the relay. The relay decodes the superimposed signals between users A and B level-by-level in the lattice, aiming to deduce the network-coded messages from the two end users. The procedures are summarized as follows:

- **Decode the network-coded message at level 1.**

The decoder at relay R decodes the signal at the first level of the lattice as follows:

$$\mathbf{y}_{R,PNC}^{(1)} = \text{mod}_\phi(\mathbf{y}_{R,PNC}), \quad (22)$$

where $\text{mod}_\phi(\mathbf{y}_{R,PNC})$ denotes $\mathbf{y}_{R,PNC}$ modulo ϕ . Through the modulo operation in (22), the resulting signal $\mathbf{y}_{R,PNC}^{(1)}$ only contains information from the first level of lattice, i.e., $\text{mod}_\phi(\mathbf{c}_{A,1} + \mathbf{c}_{B,1})$, in which the effective information $\text{mod}_\phi(\mathbf{c}_{A,1} + \mathbf{c}_{B,1})$ is a BPSK modulated signal. Then, $\mathbf{y}_{R,PNC}^{(1)}$ is sent to the channel decoder at the first level of the lattice to estimate the network-coded source information $\mathbf{s}_{R,PNC}^{(1)}$. Note that the channel decoder should be well-matched to the channel encoder at the each level of the lattice so that the decoding process can be successful. In addition, at each level of lattice, we directly apply the current PNC channel decoders where BPSK modulation is assumed, e.g., the LDPC channel decoder, convolutional codes channel decoder, and polar codes channel decoder [20]–[22]. To facilitate the decoding process in the rest levels, $\mathbf{s}_{R,PNC}^{(1)}$ is re-encoded, and the output codeword is $\mathbf{c}_{R,PNC}^{(1)}$.

- **Decode the network-coded message from level 2 to level $L_B - 1$ sequentially.**

Denote the estimated network-coded source information at level l in the lattice by $\mathbf{s}_{R,PNC}^{(l)}$, and the corresponding codeword by $\mathbf{c}_{R,PNC}^{(l)}$, $l = 2, \dots, L_B - 1$. Then, $\mathbf{s}_{R,PNC}^{(l)}$ at the level l is computed as follows:

$$\mathbf{y}_{R,PNC}^{(l)} = \text{mod}_\phi(\hat{\mathbf{y}}_{R,PNC}^{(l)}), l = 2, \dots, L_B - 1, \quad (23)$$

where

$$\begin{aligned} \hat{\mathbf{y}}_{R,PNC}^{(l)} &= \frac{1}{\phi^{l-1}} \left(\mathbf{y}_{R,PNC} - \mathbf{c}_{R,PNC}^{(1)} - \dots - \phi^{l-2} \mathbf{c}_{R,PNC}^{(l-1)} \right) \\ &= \frac{1}{\phi^{l-1}} \left(\mathbf{x}_{A,PNC} + \mathbf{x}_{B,PNC} - \mathbf{c}_{R,PNC}^{(1)} - \dots - \phi^{l-2} \mathbf{c}_{R,PNC}^{(l-1)} \right) + \frac{1}{\phi^{l-1}} \mathbf{n}_{R,PNC}. \end{aligned} \quad (24)$$

The $\mathbf{y}_{R,PNC}^{(l)}$ contains information of $\text{mod}_\phi(\mathbf{c}_{A,l} + \mathbf{c}_{B,l})$, and is then sent to the channel decoder at the level l of the lattice to estimate the network-coded source information $\mathbf{s}_{R,PNC}^{(l)}$. Next, $\mathbf{s}_{R,PNC}^{(l)}$ is re-encoded through the channel encoder at the level l of the lattice, and the output codeword is $\mathbf{c}_{R,PNC}^{(l)}$. We compute $\mathbf{c}_{R,PNC}^{(l)}$ from $l = 2$ to $l = L_B - 1$ sequentially. In addition,

in (24), since $\frac{1}{\phi^{l-1}}\mathbf{n}_{R,PNC} \sim \mathcal{CN}(\mathbf{0}, \frac{1}{2^{l-1}}\sigma_{R,PNC}^2\mathbf{I})$, the noise power decreases exponentially as l . In this case, through the operation in (23), the channel becomes a binary-input AWGN (BAWGN) channel at level l , and the capacity of the BAWGN increases as l . Thus, we can transmit much more information at higher levels of the lattice. In particular, when the lattice level l is large, the capacity of the BAWGN at the lattice level l can approach to 1.

In Fig. 4, we show the decoding process at relay R when $L_A = 3$ and $L_B = 4$ as a illustrative example. Last, the relay encodes the estimated network-coded messages, and broadcasts them to the end users.

C. Power Shaping Design

In this subsection, we show the power shaping design. To make the every dimension of the transmitted signal \mathbf{x}_u power constrained, $u \in \{A, B\}$, we apply the hypercube power shaping [14] in our PNC lattice construction in (20). Specifically, in (20), denote

$$\mathbf{c}_u = \mathbf{c}_{u,1} + \phi\mathbf{c}_{u,2} + \dots + \phi^{L_u-2}\mathbf{c}_{u,L_u-1}, u \in \{A, B\}. \quad (25)$$

Then, the hypercube power shaping is expressed as follows:

$$\mathbf{b}_u = \frac{1}{\phi^{L_u-1}} (\text{mod}_{\phi^{L_u-1}}(\mathbf{c}_u) - \mathbf{c}_u), u \in \{A, B\}. \quad (26)$$

In this case, the transmitted packet at user u is

$$\mathbf{x}_{u,PNC} = \mathbf{c}_{u,1} + \phi\mathbf{c}_{u,2} + \dots + \phi^{L_u-2}\mathbf{c}_{u,L_u-1} + \phi^{L_u-1}\mathbf{b}_u \quad (27)$$

$$= \text{mod}_{\phi^{L_u-1}}(\mathbf{c}_u), u \in \{A, B\}. \quad (28)$$

Thus, the power shaping makes the every dimension of the transmitted signal $\mathbf{x}_{u,PNC}$ power constrained, $u \in \{A, B\}$. For example, when $L_A = 3$, $x_{A,PNC}^{(n)} \in \{0, j, -1, -1 - j\}$; when $L_A = 4$, $x_{A,PNC}^{(n)} \in \{0, j, -1, -1 - j, -j, 1, 1 - j, -2j\}$, where $x_{A,PNC}^{(n)}$ is the n -th element of $\mathbf{x}_{A,PNC}$, $n = 1, \dots, N$.

In lattice construction, only hypercube power shaping design shown above can make the transmitted signals power constrained. The lattice applying hypercube power shaping works well in point to point communications, and in PNC when $L_A = L_B$. However, in PNC when $L_B > L_A$ is studied in this paper, the hypercube power shaping causes decoding failure at the relay for lattice levels $l \geq L_A$ when $\text{mod}_{\phi}(\mathbf{b}_A)$ is not a codeword to the codebook at the lattice level L_A . Specifically, in (21), at level L_A in the lattice, the signal $\mathbf{y}_{R,PNC}^{(L_A)}$ contains information of

$$\text{mod}_{\phi}(\mathbf{b}_A + \mathbf{c}_{B,L_A}) = \text{mod}_{\phi}(\text{mod}_{\phi}(\mathbf{b}_A) + \mathbf{c}_{B,L_A}). \quad (29)$$

Based on $\mathbf{y}_{R,PNC}^{(L_A)}$, the decoder applies channel decoder to recover the signal $\text{mod}_\phi(\mathbf{b}_A + \mathbf{c}_{B,L_A})$. The problem is, $\text{mod}_\phi(\mathbf{b}_A)$ may not be a codeword to the codebook at the lattice level L_A , i.e., the channel decoder cannot decode $\text{mod}_\phi(\mathbf{b}_A)$ successfully even in the absence of noise. When $\text{mod}_\phi(\mathbf{b}_A)$ is not a codeword, the superimposed signal $\text{mod}_\phi(\mathbf{b}_A + \mathbf{c}_{B,L_A})$ may also not a codeword of the codebook at the lattice level L_A . Thus, the decoder at the level L_A can not recover $\text{mod}_\phi(\mathbf{b}_A + \mathbf{c}_{B,L_A})$, even in the absence of noise. Moreover, the decoding errors are propagated to the decoders at the lattice levels $l > L_A$.

To solve the problem, we need to find a way that can not only make the transmitted signal power constrained by applying the power shaping in (26), but also make the decoding in the level L_A successfully. To this end, denote \mathbf{c}_{A,L_A} a codeword of the codebook at the lattice level L_A . In this case, we propose to ask user A to transmit a correction signal $\mathbf{e} \in \{0, 1\}^N$ to the relay beforehand such that

$$\text{mod}_\phi(\mathbf{c}_{A,L_A}) = \text{mod}_\phi(\mathbf{b}_A - \mathbf{e}). \quad (30)$$

Then, users A and B transmit their signals to the relay simultaneously. Upon receiving the superimposed signals $\mathbf{y}_{R,PNC}$ as shown in (21), the correction signal $\mathbf{e} \in \{0, 1\}^N$ is subtracted from $\mathbf{y}_{R,PNC}$, and the resulting signal is

$$\begin{aligned} \hat{\mathbf{y}}_{R,PNC} &= \mathbf{y}_{R,PNC} - \phi^{L_A-1} \mathbf{e} = \mathbf{x}_{A,PNC} + \mathbf{x}_{B,PNC} - \phi^{L_A-1} \mathbf{e} + \mathbf{n}_{R,PNC} \\ &= (\mathbf{c}_{A,1} + \mathbf{c}_{B,1}) + \cdots + \phi^{L_A-2} (\mathbf{c}_{A,L_A-1} + \mathbf{c}_{B,L_A-1}) \\ &\quad + \phi^{L_A-1} (\mathbf{b}_A - \mathbf{e} + \mathbf{c}_{B,L_A}) + \cdots + \phi^{L_B-1} \mathbf{b}_B + \mathbf{n}_{R,PNC}. \end{aligned} \quad (31)$$

In this case, at the level L_A , according to (30), since

$$\text{mod}_\phi(\mathbf{b}_A - \mathbf{e} + \mathbf{c}_{B,L_A}) = \text{mod}_\phi(\mathbf{c}_{A,L_A} + \mathbf{c}_{B,L_A}) \quad (32)$$

is a codeword to the codebook at the lattice level L_A , the decoder can recover $\text{mod}_\phi(\mathbf{c}_{A,L_A} + \mathbf{c}_{B,L_A})$ successfully through the decoding and encoding process. In this case, the transmitted signals at the two users are power constrained, and the relay can decode the superimposed signals successfully. There are two problems to be solved:

Problem A: Find a codeword around the hypercube power shaping. From (30), we have

$$\text{mod}_\phi(\mathbf{b}_A) = \text{mod}_\phi(\text{mod}_\phi(\mathbf{c}_{A,L_A}) + \mathbf{e}). \quad (33)$$

We can imagine that the codeword $\text{mod}_\phi(\mathbf{c}_{A,L_A})$ goes through a binary symmetric channel (BSC) with bit flipping probability p , the correction signal \mathbf{e} is the corresponding BSC noise, and $\text{mod}_\phi(\mathbf{b}_A)$

is the output of the BSC channel. The capacity C_{BSC} of the BSC is [23]

$$C_{BSC} = 1 - H(p), \quad (34)$$

where

$$H(p) = -p \log_2(p) - (1 - p) \log_2(1 - p), \quad (35)$$

is the entropy of e_n with e_n being the n -th element of e , $n = 1, \dots, N$. To find the codeword \mathbf{c}_{A,L_A} , we send $\text{mod}_\phi(\mathbf{b}_A)$ to the BSC channel decoder with the output source information \mathbf{s}_{A,L_A} . The BSC channel decoder is similar to the channel decoder at the lattice level L_A , and the only difference is that the channel decoder is constructed under binary AWGN channel, while the BSC channel decoder is constructed under BSC channel. The source information \mathbf{s}_{A,L_A} is then re-encoded, with output codeword \mathbf{c}_{A,L_A} . The correction signal (i.e., the BSC noise) e is

$$\mathbf{e} = \text{mod}_\phi(\mathbf{b}_A - \mathbf{c}_{A,L_A}). \quad (36)$$

The above decoding process, i.e., finding $\text{mod}_\phi(\mathbf{c}_{A,L_A})$ from $\text{mod}_\phi(\mathbf{b}_A)$ with e being the noise vector, can be interpreted as a lossy compression process. We denote the space $\text{mod}_\phi(\mathbf{c}_{A,L_A})$ lies in by $\{0, 1\}^{K_{L_A}}$, i.e., the dimension of the space is K_{L_A} although the length of the codeword \mathbf{c}_{A,L_A} is N , and the space $\text{mod}_\phi(\mathbf{b}_A)$ lies in by $\{0, 1\}^N$. In this case, the BSC decoding process actually compresses the space $\{0, 1\}^N$ to the space $\{0, 1\}^{K_{L_A}}$. Ref. [24] proves that, as N goes to infinity, for the lossy compression under the measure of Hamming distortion, the optimal compression rate can be expressed as

$$\frac{K_{L_A}}{N} = R_{L_A} = 1 - H(p), \quad (37)$$

where $H(p)$ is the entropy of e . In this case, we can determine the flipping probability according to (37).

B: Compress the correction signal e in (36) by applying lossless polar source coding. To facilitate the decoding process in the relay as shown in (31), we need to transmit the correction signal e in (36) to the relay. However, if we ask the user A to transmit the correction signal e with length $K_e = N$ directly, the time saved through the asymmetric PNC transmission will be canceled out by the correction signal transmission. Fortunately, according to (37), if the rate R_{L_A} is large, then the entropy of e would be small. In this case, we can apply the lossless polar source coding [15] to compress the correction signal e . Specifically, according to [15], as N goes to infinity, the compression rate is $H(p)$ shown in (35). In this case, we can transmit the compressed correction signal \hat{e} with

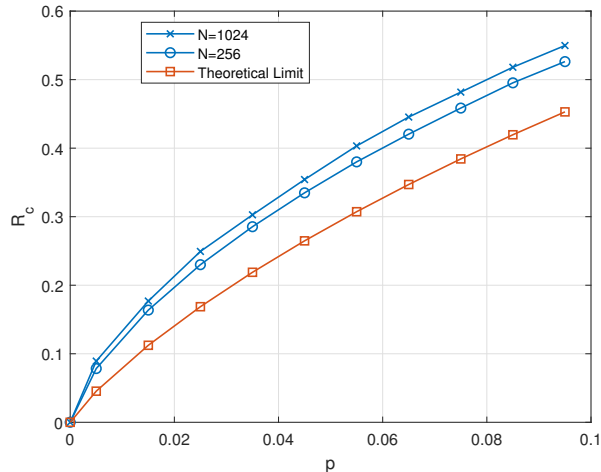


Fig. 5. Compression rate R_c over flipping probability p for different N .

the length $K_{\hat{e}} = NH(p)$ instead of the original correction signal e with length $K_e = N$, greatly saving the correction signal transmission time. In practice, for N is finite, we apply the lossless polar source coding algorithm proposed in [16]. According to the algorithm, we can perfectly recover e from \hat{e} , and e is plugged into (31) for PNC decoding. The algorithm details are omitted.

In Fig. 5, we show the compression rate

$$R_c = \frac{K_{\hat{e}}}{N} \quad (38)$$

The theoretical limit is $R_c = H(p)$ shown in [15], and the other two lines show the results in [16] for packet length $N = 256$ and $N = 1024$. Fig. 5 shows that, when the flipping probability is small, we can reduce the length of the correction signal e significantly by applying the lossless polar source coding. In addition, as the packet length N becomes large, the compression rate in [16] approaches to the theoretical limit.

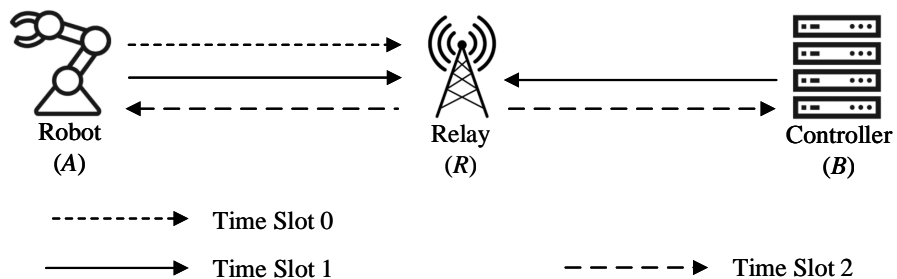


Fig. 6. Overall asymmetric transmission scheme with correction signal transmission taken into account.

D. Overall Asymmetric Transmission Scheme

The overall asymmetric transmission scheme is shown in Fig. 6. The signal transmission processes are detailed as follows.

Time slot 0: Compressed correction signal \hat{e} transmission. The user A first computes the correction signal e according to the method introduced in Section III-C, then compresses the correction signal by applying lossless polar source coding according to the algorithm in [16]. Next, user A transmits the compressed correction signal to the relay. We assume that the user A applies a channel-encoder-and-modulator with coding rate $R_{A,P2P}$ and modulator order M_A to transmit the source information \hat{e} . The modulator order is restricted by the weaker channel h_A to achieve a targeted FER. The transmit packet is $\mathbf{x}_{A,P2P}$, and duration of the correction signal transmission is

$$T_{\hat{e}} = \frac{K_{\hat{e}}}{R_{A,P2P}M_AW}. \quad (39)$$

At the relay R , the received signal is

$$\mathbf{y}_{R,P2P} = \mathbf{x}_{A,P2P} + \mathbf{n}_{R,P2P}, \quad (40)$$

where $\mathbf{n}_{R,P2P} \sim \mathcal{CN}(\mathbf{0}, \sigma_{R,P2P}^2 \mathbf{I})$ denotes the additive white Gaussian noise (AWGN) at the relay in the P2P phase. Note that, the channel h_A has been compensated at the relay. The decoder at the relay R first decodes the compressed correction signal \hat{e} , and then decompressed it to recover the original correction signal e by applying the algorithm in [16].

Time slot 1: Uplink PNC transmission. The encoding and modulation processes are the same as that introduced in Section II-B. To solve the problem that the users A and B can transmit different amount of information, we apply the lattice-based channel-encoder-and-modulator shown in Section III-B. In addition, to make the decoding at the relay successfully, the estimated correction signal is subtracted from the received signal, and the resulting received signal is shown in (31). Moreover, we apply the lattice-based channel-decoder-and-demodulator to estimate the network-coded messages shown in III-B.

Time slot 2: Downlink PNC transmission. The encoding and decoding processes are the same as that introduced in Section II-B.

In this case, the total transmission time of the asymmetric transmission scheme in (14) is rewritten as

$$\hat{T}^{(Asy)} = T_1^{(Asy)} + T_2^{(Asy)} + T_{\hat{e}} = \frac{K_A}{R_{A,PNC}M_AW} + \frac{K_B}{R_{R,PNC}M_AW} + \frac{K_{\hat{e}}}{R_{A,P2P}M_AW}. \quad (41)$$

If we set $R_{R,PNC} = R_{R,P2P}$, from (11) and (41), we have

$$T^{(Sym)} - \hat{T}^{(Asy)} = T_3^{(Sym)} - T_{\hat{e}} = \frac{K_B - K_A}{R_{B,P2P}M_BW} - \frac{K_{\hat{e}}}{R_{A,P2P}M_AW}. \quad (42)$$

Remark 1: As we discussed in Section III-B, as the increase of the lattice level l , the capacity of the BAWGN increases even approaching to 1. In this case, the coding rate R_{L_A} can approach to 1 potentially. Then, according to (37), we know that $H(p)$ approaches to zero as the increase of the lattice level. In this case, we can compress the signal e to \hat{e} with length $K_{\hat{e}} = NH(p)$ approaching to zero when L_A is large enough, and the correction signal transmission time $T_{\hat{e}}$ can be far smaller than $T_3^{(Sym)}$. In particular, if the coding rate $R_{L_A} = 1$, we have $T_{\hat{e}} = 0$. We show this case though the example when user A applies 3-order modulation, and user B applies 4-order modulation in Section IV.

Moreover, to make the study of the asymmetric comprehensive, we also consider the case when the coding rate R_{L_A} is not close to 1. In this case, the length of the compressed correction signal \hat{e} would be large, and may leading to the transmission time $T_{\hat{e}}$ larger than $T_3^{(Sym)}$. In this case, the throughput of the proposed asymmetric transmission scheme may be smaller than that of the symmetric transmission. We solve this problem in Section V.

IV. NUMERICAL RESULTS

In this section, we evaluate performance of the proposed asymmetric transmission scheme detailed in Section II-B. Specifically, in the simulations, we assume that the modulation orders $M_A = 3$, and $M_B = 4$, i.e., the channel h_A can support user A to transmit signals with modulation order of 3, and the channel h_B can support user B to transmit signals with modulation order of 4. In addition, as an example, we apply the polar codes for lattice construction. The results of this section can be extended to the case where the other channel error correcting codes are applied. We omit the details here. In the asymmetric transmission scheme, we apply lattice-based channel-encoder-and-modulator shown in Section III, both for uplink and downlink PNC transmissions, and the correction signal \hat{e} transmission in the asymmetric transmission scheme. Note that the downlink PNC transmission and the correction signal transmission are simple P2P transmissions, and the lattice-based encoding and decoding algorithms shown in Section III can be applied directly. In the simulations, we denote this scheme by “**Asymmetric transmission applying Lattice-based channel-Encoder-and-Modulator (ALEM)**”. We have the following two benchmarks:

- **Symmetric transmission applying Lattice-based channel-Encoder-and-Modulator (SLEM):**

We apply lattice-based channel-encoder-and-modulator both for uplink and downlink transmis-

sions in the time slots 1 to 4 in the symmetric transmission scheme detailed in Section II-A. Specifically, for time slot 1, i.e., the uplink of PNC transmission, the lattice encoding and decoding processes in the symmetric transmission scheme are similar to that introduced in Section III-B by simply setting $L_A = L_B$. In addition, since $L_A = L_B$, we do not need to transmit correction signals beforehand. Moreover, the transmissions in time slots 2-4 are simple P2P transmissions, and the lattice-based encoding and decoding algorithms shown in Section III can be applied directly.

- **Symmetric transmission applying Traditional channel-Encoder-and-Modulator (STEM):** Unlike SLEM above, in this symmetric transmission scheme, we apply a traditional channel-encoder-and-modulator, in which a channel encoder is followed by a signal modulator. In this case, the channel encoding and modulation are two separately processes, which is different from the the joint channel encoding and modulation in the lattice-based scheme. Specifically, in the traditional channel-encoder-and-modulator, we apply the polar codes, and 8QAM and 16QAM modulation, depending on the required modulation order in each time slot. Moreover, in time slot 1 of the symmetric transmission, i.e., the uplink transmission of PNC, the relay applies a XOR channel decoder [22] to decode the network-coded messages from the two users. The XOR channel decoder is quite similar to that introduced in Section II-D.

We evaluate the performance in terms of FER and throughput of user B . The throughput is defined as follows:

$$\text{Throughput} = \frac{P_B K_B}{T} \text{ bps} \quad (43)$$

where P_B is the number of successful received packets transmitted from user B at user A ; K_B is the number of information bits per packet; and T is the transmission duration. In the symmetric transmission, $T = T^{(Sym)}$ shown in (11), and in the asymmetric transmission, $T = T^{(Asy)}$ shown in (41). The unit is bits per second (bps). In addition, the bandwidth is 1 M symbols/second. Moreover, the SNR is defined in the uplink of PNC in the asymmetric transmission scheme. Specifically,

$$SNR = \frac{p_B N}{K_B N_0} \quad (44)$$

where p_B is the uplink transmit power of user B , N is the transmitted packet length in the uplink of PNC, and $N_0 = 2\sigma_{R,PNC}^2$ is the noise power. In addition, in the simulations, we set $\sigma_{R,PNC}^2 = \sigma_{u,PNC}^2 = \sigma_{R,P2P}^2 = \sigma_{u,P2P}^2$, $u \in \{A, B\}$.

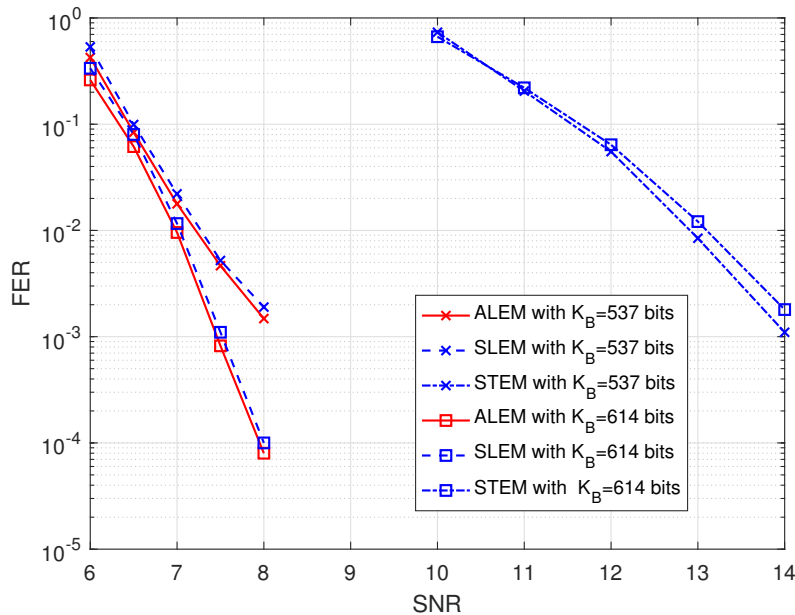


Fig. 7. FER comparison when $\text{mod}_\phi(\mathbf{b}_A)$ is a legal codeword.

A. Performance When $\text{mod}_\phi(\mathbf{b}_A)$ is a Codeword

In the asymmetric transmissions in which $L_A < L_B$, in Section III-C we show that the hypercube power shaping may cause decoding failures at the relay when the power shaping modulo ϕ at user A , i.e., $\text{mod}_\phi(\mathbf{b}_A)$, is not a codeword to the codebook at the lattice level L_A . In this subsection, we first evaluate the performance of the asymmetric transmission in which $\text{mod}_\phi(\mathbf{b}_A)$ is a codeword to the codebook at the lattice level L_A by simply setting the rate in lattice level- L_A as 1, i.e., $R_{L_A} = 1$. In this case, since the codebook in lattice level- L_A is exactly the space $\{0, 1\}^N$, where N is the codeword length, $\text{mod}_\phi(\mathbf{b}_A)$ is a legal codeword to the codebook. As a result, we do not need to transmit the correction signal e in the asymmetric transmissions.

We show the results in Figs. 7 and 8. Let us first introduce the legends in the figures as follows:

- **ALEM with $K_B = 537$ bits:** In the uplink of PNC, user B applies a 5-level lattice, with coding rates $R_1 = 0.003$, $R_2 = 0.45$, $R_3 = 0.65$, and $R_4 = 1$, respectively. The packet length is $N = 256$ for all levels. In this case, user B transmits $K_B = 537$ bits in total. In the downlink of PNC, the relay applies a 4-level lattice to broadcast the network-coded information, with coding rates $R_1 = 0.003$, $R_2 = 0.45$, and $R_3 = 0.65$, respectively. Since $R_4 = 1$, we do not need to transmit the correction signals beforehand.
- **ALEM with $K_B = 614$ bits:** The setup is the same as “ALEM with $K_B = 537$ bits” except that the coding rate in the lattice level-3 is $R_3 = 0.95$. In this case, user B transmits $K_B = 614$

bits in total.

- **SLEM with $K_B = 537$ bits:** In time slot 1, i.e., the uplink of PNC, user B applies a 4-level lattice, with coding rates $R_1 = 0.003$, $R_2 = 0.45$, and $R_3 = 0.65$, respectively. The packet length is $N = 256$ for all levels. In this case, user B transmits 281 bits; In time slot 2, i.e., the downlink of PNC, the rate setup is the same as that in the uplink of PNC; in time slot 3, the user B applies a 5-level lattice, with coding rates $R_1 = 0.003$, $R_2 = 0.45$, $R_3 = 0.65$, and $R_4 = 1$, respectively, to transmit the rest of 256 bits to the relay; in time slot 4, the relay applies a 4-level lattice, with coding rate $R_1 = 0.003$, $R_2 = 0.45$, and $R_3 = 0.65$, respectively, to transmit the message to user A . In this case, user B transmits $K_B = 537$ bits in total.
- **SLEM with $K_B = 614$ bits:** The setup is the same as “SLEM with $K_B = 537$ bits” except that the coding rate in the lattice level-3 is $R_3 = 0.95$ in the time slots 1 to 4. Thus, user B transmits $K_B = 614$ bits in total.
- **STEM with $K_B = 537$ bits:** In time slot 1, i.e., the uplink of PNC, user B applies polar codes with coding rate $R_{B,PNC} = (0.003 + 0.45 + 0.65)/3 = 0.37$ to transmit 281 bits source information. In time slot 2, i.e., the downlink of PNC, the rate setup is the same as the uplink of PNC; in time slot 3, user B applies polar codes with coding rate $R_{B,P2P} = (0.003 + 0.45 + 0.65 + 1)/4 = 0.53$ to transmit the rest of 256 bits to the relay; in time slot 4, the relay applies polar codes with coding rate $R_{R,P2P} = (0.003 + 0.45 + 0.65)/3 = 0.37$ to transmit the message to user A . In this case, user B transmits $K_B = 537$ bits in total.
- **STEM with $K_B = 614$ bits:** The setup is the same as “STEM with $K_B = 537$ bits” except that the coding rates now are $R_{B,PNC} = (0.003 + 0.45 + 0.95)/3 = 0.47$, $R_{B,P2P} = (0.003 + 0.45 + 0.95 + 1)/4 = 0.60$, and $R_{R,P2P} = (0.003 + 0.45 + 0.95)/3 = 0.47$. In this case, user B transmits $K_B = 614$ bits in total.

From Fig. 7, we know that for the same amount of the transmitted bits K_B , the FERs of ALEM and SLEM are roughly the same. In addition, Fig. 7 shows that, for a given SNR, ALEM/SLEM with $K_B = 614$ bits performs better than that with $K_B = 537$ bits. The reason is as follows. From (44), for a given SNR, the product of the coding rate and the noise power is fixed. The coding rate of ALEM with $K_B = 537$ is lower than ALEM with $K_B = 614$ bits in the uplink and downlink of PNC respectively, since ALEM with $K_B = 537$ bits transmits less information. Similar observations also applied to SLEM with $K_B = 537$ bits and with $K_B = 614$ bits. In this case, although the coding rate of ALEM/SLEM with $K_B = 537$ bits is lower than that of ALEM/SLEM with $K_B = 614$ bits, Fig. 7 shows that the noise have much more negative influence on ALEM/SLEM with $K_B = 537$ bits. As a result, ALEM/SLEM with $K_B = 537$ bits performs

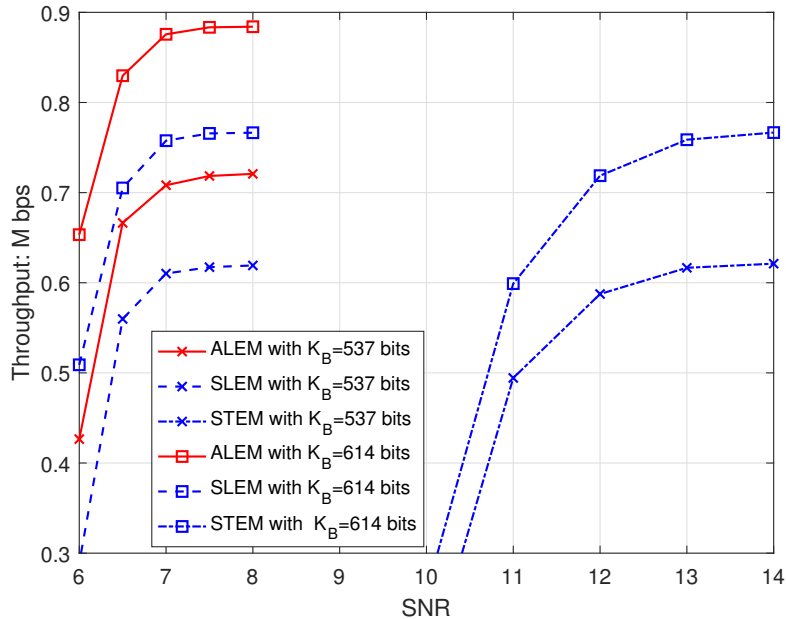


Fig. 8. Throughput comparison when $\text{mod}_\phi(\mathbf{b}_A)$ is a legal codeword.

worse than ALEM/SLEM with $K_B = 614$ bits. Moreover, Fig. 8 shows that, in terms of throughput, ALEM performs much better than SLEM. For example, when $SNR = 8$ dB, ALEM with $K_B = 614$ bits has 15.3% throughput improvement compared with that of SLEM with $K_B = 614$ bits. It suggests that, our proposed asymmetric transmission scheme has significant throughput improvement compared with that of the symmetric transmission, since the asymmetric transmission scheme saves the transmission time greatly. In addition, the asymmetric transmission scheme, i.e., ALEM, can achieve the above throughput improvement by simply setting the coding rate $R_{L_A} = 1$.

Next, we compare the performance of SLEM and STEM. From Fig. 7, for a given FER, SLEM performs 6 dB better than that of STEM. The reasons mainly come from the decoder at the relay in the uplink of the PNC stage. Specifically, for a given SNR, the PNC detector for low-order modulated signals has better FER performance than that for high-order modulated signals [22]. For example, the detector for BPSK-modulated signals performs better than the detector for 8QAM-modulated signals in terms of FER. From the decoding process detailed in Section III-B, for SLEM the signals fed to the decoder at each level of the lattice are BPSK-modulated through the modulo ϕ operation, while for STEM the signals fed to the detector are 8QAM modulated. As a result, SLEM performs better than STEM. From Fig. 8, the throughput of SLEM is much higher than that of STEM, since the FER of SLEM is much lower than that of STEM.

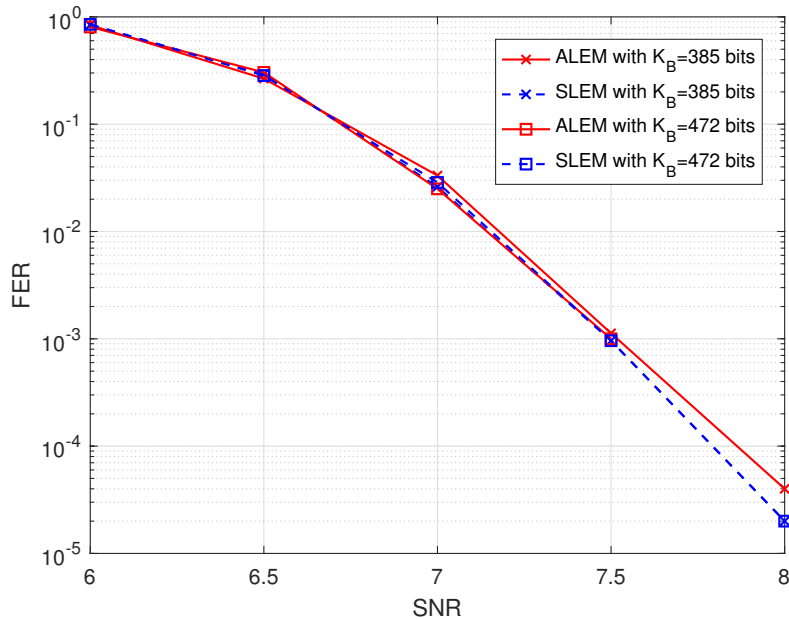


Fig. 9. FER comparison for general hypercube power shaping.

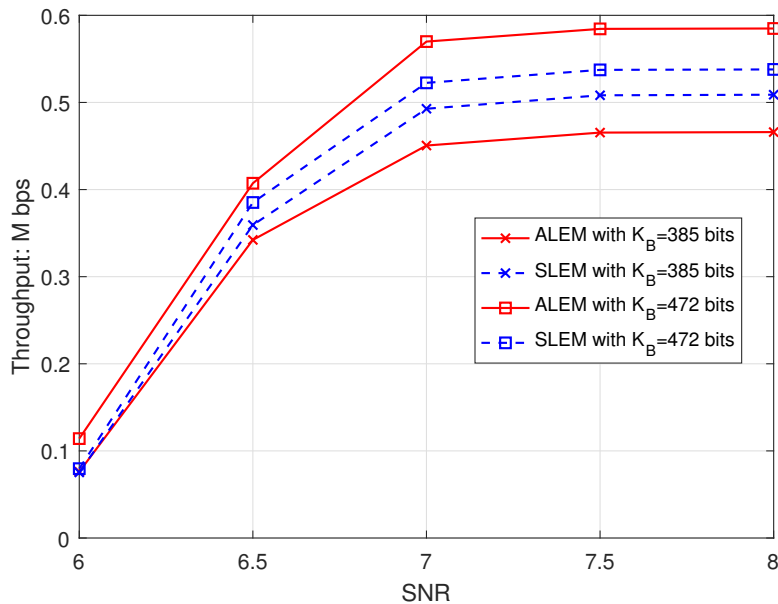


Fig. 10. Throughput comparison for general hypercube power shaping.

B. Performance for General Hypercube Power Shaping

We next show the simulation results for general hypercube power shaping in Figs.9-11. Let us first introduce the legends in the figure, as follows:

- **ALEM with $K_B = 385$ bits:** The user A first transmits the compressed correction signal \hat{e} with the length $K_{\hat{e}}$ to the relay. It applies a 4-level lattice, with coding rates $R_1 = 0.003$, $R_2 = 0.40$,

and $R_3 = 0.55$. The rest of the setup is the same as “ALEM with $K_B = 537$ bits” introduced in Section IV-A except that the coding rates now are $R_1 = 0.003$, $R_2 = 0.40$, $R_3 = 0.55$, and $R_4 = 0.56$. In this case, user B transmits $K_B = 385$ bits in total.

- **ALEM with $K_B = 472$ bits:** The setup is the same as “ALEM with $K_B = 385$ bits” introduced above except that the coding rate R_4 now is $R_4 = 0.90$. In this case, user B transmits $K_B = 472$ bits in total.
- **SLEM with $K_B = 385$ bits:** The setup is the same as “SLEM with $K_B = 537$ bits” introduced in Section IV-A except that the coding rates now are $R_1 = 0.003$, $R_2 = 0.40$, $R_3 = 0.55$, and $R_4 = 0.56$. In this case, user B transmits $K_B = 385$ bits in total.
- **SLEM with $K_B = 472$ bits:** The setup is the same as “SLEM with $K_B = 385$ bits” introduced above except that the coding rate R_4 now is $R_4 = 0.90$. In this case, user B transmits $K_B = 472$ bits in total.

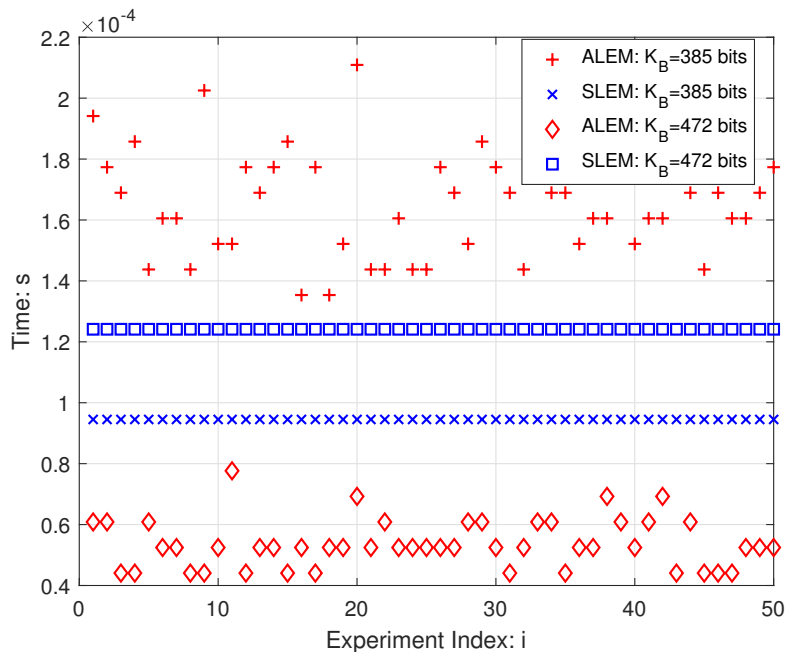


Fig. 11. $T_3^{(Sym)}$ and $T_{\hat{e}}$ comparison over different K_B . In ALEM, we plot the time $T_{\hat{e}}$ for $K_B = 385$ bits and $K_B = 472$ bits; in SLEM, we plot the time $T_3^{(sym)}$ for $K_B = 385$ bits and $K_B = 472$ bits.

From Fig. 9, we observe that ALEM and SLEM perform relative the same. Fig. 10 shows that ALEM with $K_B = 472$ bits outperforms SLEM with $K_B = 472$ bits, while ALEM with $K_B = 385$ bits performs worse than SLEM with $K_B = 385$ bits. The reasons are shown in Fig. 11. Specifically, in Fig. 11, we compare $T_3^{(Sym)}$ and $T_{\hat{e}}$ over different K_B for 50 Monte Carlo simulations. When $K_B = 472$ bits, the time for correction signal transmission in ALEM is smaller than the duration in time slot 3 in SLEM, i.e., $T_{\hat{e}} < T_3^{(Sym)}$. As a result, from (42), the asymmetric transmission time is

less than that of the symmetric transmission time, i.e., $T^{(Asy)} < T^{(Sym)}$. In this case, for the relatively same FER, AELM performs better than SLEM when $K_B = 472$ bits. When $K_B = 385$ bits, the time for correction signal transmission in AELM is larger than the duration in time slot 3 in SLEM, i.e., $T_{\hat{e}} > T_3^{(Sym)}$ since the coding rate R_4 is far smaller than 1. As a result, from (42), the asymmetric transmission time is larger than that of the symmetric transmission time, i.e., $T^{(Asy)} > T^{(Sym)}$. In this case, for the relatively same FER, SLEM performs better than AELM when $K_B = 385$ bits.

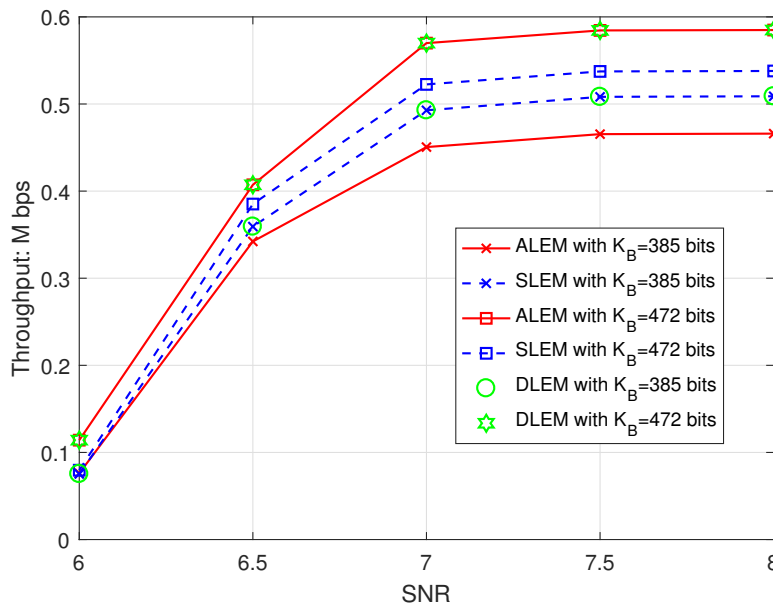


Fig. 12. Throughput comparison between DLEM, ALEM, and SLEM for general hypercube power shaping.

V. DYNAMIC TRANSMISSION SCHEME

As we discussed in Remark 1, and shown in Section IV-B, when the coding rate R_{L_A} is far smaller than 1, the symmetric transmission may perform better than that of the asymmetric transmission since $T_{\hat{e}} > T_3^{(Sym)}$. In this case, if we insist on asymmetric transmission all the time, we will not achieve the optimal throughput in the end since sometimes the symmetric transmission scheme performs better. To solve the above problem, we propose to ask the relay R to choose the two schemes dynamically based on the values of $T_{\hat{e}}$ and $T_3^{(Sym)}$ so that the dynamic transmission scheme can always achieve the better performance between ALEM and SLEM. Specifically, if $T_3^{(Sym)} \leq T_{\hat{e}}$, then the symmetric transmission scheme is selected; otherwise, the asymmetric transmission scheme is selected. We denote this scheme by “**Dynamic transmission scheme applying Lattice-based channel-Encoder-and-Modulator (DLEM)**”. The simulation results are shown in Fig. 12. Let us first introduce the legends as follows.

- **DLEM with $K_B = 385$ bits:** The relay dynamic selects the scheme between “ALEM with $K_B = 385$ bits” and “SLEM with $K_B = 385$ bits” according to the values $T_{\hat{e}}$ and $T_3^{(Sym)}$. The “ALEM with $K_B = 385$ bits” and “SLEM with $K_B = 385$ bits” are introduced in Section IV-B.
- **DLEM with $K_B = 472$ bits:** The relay dynamic selects the scheme between “ALEM with $K_B = 472$ bits” and “SLEM with $K_B = 472$ bits” according to the values $T_{\hat{e}}$ and $T_3^{(Sym)}$. The “ALEM with $K_B = 472$ bits” and “SLEM with $K_B = 472$ bits” are introduced in Section IV-B.

Fig. 12 shows the simulation results when applying the dynamic transmission scheme. As a result, since DLEM always choose the scheme with smaller transmission time, DLEM always achieves the better performance between SLEM and ALEM over different rate setups.

VI. CONCLUSION

This paper studied the asymmetric transmission scheme in PNC in which the users A and B transmit different amount of information in the uplink of PNC simultaneously. A key challenge is how to do channel coding in asymmetric PNC transmission such that the relay can deduce meaningful network-coded messages from the two users. To solve this problem, we proposed a lattice based channel-encoder-and-modulator in which the two users encode and modulate their information in lattices with different levels. In addition, to make every dimension of the lattice power constrained, we applied hypercube power shaping. However, the hypercube power shaping causes decoding failures at the relay since the hypercube power shaping is not a legal codeword to the codebook at lattice level L_A in general. We solved this problem by asking user A to transmit a correction signal beforehand such that the difference between the power shaping and the correction signal is a legal codeword. Upon receiving the superimposed signal, the correction signal is subtracted from the received signal.

To reduce the correction signal transmission time, we applied the polar source coding technique to compress the correction signal and we transmit the compressed correction signal instead. We find that the polar source coding technique can efficiently reduce the correction signal transmission time when the channel coding rate at lattice level L_R is close to 1. In addition, we also considered the case where channel coding rate at lattice level L_R is not close to 1. In this case, the length of the compressed correction signal may be large, and the asymmetric transmission scheme may spend much time on the correction signal transmission in addition to the PNC transmission. Thus, the overall asymmetric transmission time may be larger than the symmetric time. To solve this problem, we put forth a dynamic transmission scheme in which the relay dynamically selects one of the transmission schemes which has smaller transmission time. Numerical results demonstrate the effectiveness of the proposed schemes.

REFERENCES

- [1] P. Varga, J. Peto, A. Franko, D. Balla, D. Haja, F. Janky, G. Soos, D. Ficzer, M. Maliosz, and L. Toka, "5G support for industrial IoT applications—challenges, solutions, and research gaps," *Sensors*, vol. 20, no. 3, p. 828, Feb. 2020.
- [2] E. Sisinni, A. Saifullah, S. Han, U. Jennehag, and M. Gidlund, "Industrial internet of things: Challenges, opportunities, and directions," *IEEE Transactions on Industrial Informatics*, vol. 14, no. 11, pp. 4724–4734, Jul. 2018.
- [3] T. YAMAMOTO and Y. OKADA, "Multi-hop wireless network for industrial IoT," *SEI TECHNICAL REVIEW*, no. 86, p. 9, Feb. 2018.
- [4] T. Kagawa, F. Ono, L. Shan, K. Takizawa, R. Miura, H.-B. Li, F. Kojima, and S. Kato, "A study on latency-guaranteed multi-hop wireless communication system for control of robots and drones," in *Proceedings of IEEE International Symposium on Wireless Personal Multimedia Communications (WPMC)*, Dec. 2017.
- [5] S. Zhang, S. C. Liew, and P. P. Lam, "Hot topic: physical-layer network coding," in *Proceedings of the 12th annual international conference on Mobile computing and networking*, Sep. 2006.
- [6] P. Popovski and H. Yomo, "Physical network coding in two-way wireless relay channels," in *Proceedings of IEEE International Conference on Communications*, Aug. 2007.
- [7] Z. Wang, "Signal detection for short-packet physical-layer network coding with FSK modulation," Ph.D. dissertation, The Chinese University of Hong Kong (Hong Kong), 2019.
- [8] L. Shi, S. C. Liew, and L. Lu, "On the subtleties of q -PAM linear physical-layer network coding," *IEEE Transactions on Information Theory*, vol. 62, no. 5, pp. 2520–2544, Mar. 2016.
- [9] L. Shi and S. C. Liew, "Complex linear physical-layer network coding," *IEEE Transactions on Information Theory*, vol. 63, no. 8, pp. 4949–4981, Apr. 2017.
- [10] Z. Wang, S. C. Liew, and L. Lu, "Noncoherent detection for physical-layer network coding," *IEEE Transactions on Wireless Communications*, vol. 17, no. 10, pp. 6901–6916, Aug. 2018.
- [11] H. Zhang and L. Cai, "Design of channel coded heterogeneous modulation physical layer network coding," *IEEE Transactions on Vehicular Technology*, vol. 67, no. 3, pp. 2219–2230, Oct. 2017.
- [12] H. Pan, L. Lu, and S. C. Liew, "Practical power-balanced non-orthogonal multiple access," *IEEE Journal on Selected Areas in Communications*, vol. 35, no. 10, pp. 2312–2327, Jul. 2017.
- [13] G. Forney, "Coset codes-part I: Introduction and geometrical classification," *IEEE Transactions on Information Theory*, vol. 34, no. 5, pp. 1123–1151, Sep. 1988.
- [14] Y. Tan, S. C. Liew, and T. Huang, "Mobile lattice-coded physical-layer network coding with practical channel alignment," *IEEE Transactions on Mobile Computing*, vol. 17, no. 8, pp. 1908–1923, Jan. 2018.
- [15] E. Arikan, "Source polarization," in *Proceedings of IEEE International Symposium on Information Theory*, Jul. 2010.
- [16] H. S. Cronie and S. B. Korada, "Lossless source coding with polar codes," in *Proceedings of IEEE International Symposium on Information Theory*, Jul. 2010.
- [17] A. Goldsmith, *Wireless communications*. Cambridge university press, 2005.
- [18] Z. Wang and S. C. Liew, "Coherent detection for short-packet physical-layer network coding with binary FSK modulation," *IEEE Transactions on Wireless Communications*, vol. 19, no. 1, pp. 279–292, Oct. 2019.
- [19] Z. Wang, S. C. Liew, and L. Lu, "Optimal noncoherent detection for physical-layer network coding," in *Proceedings of IEEE Global Communications Conference (GLOBECOM)*, Dec. 2018.
- [20] Z. Xie, P. Chen, Z. Mei, S. Long, K. Cai, and Y. Fang, "Polar-coded physical layer network coding over two-way relay channels," *IEEE Communications Letters*, vol. 23, no. 8, pp. 1301–1305, Aug. 2019.
- [21] Q. Yang and S. C. Liew, "Asynchronous convolutional-coded physical-layer network coding," *IEEE Transactions on Wireless Communications*, vol. 14, no. 3, pp. 1380–1395, Oct. 2014.
- [22] S. C. Liew, L. Lu, and S. Zhang, "A primer on physical-layer network coding," *Synthesis Lectures on Communication Networks*, vol. 8, no. 1, pp. 1–218, Jun. 2015.
- [23] T. M. Cover, *Elements of information theory*. John Wiley & Sons, 1999.
- [24] S. B. Korada and R. L. Urbanke, "Polar codes are optimal for lossy source coding," *IEEE Transactions on Information Theory*, vol. 56, no. 4, pp. 1751–1768, Mar. 2010.